Inorg. Chem. **2008**, *47*, 8553−8561

Forum

Transition-Metal Oxides with Triangular Lattices: Generation of New Magnetic and Electronic Properties

A. Maignan,* W. Kobayashi, S. Hébert, G. Martinet, D. Pelloquin, N. Bellido, and Ch. Simon

Laboratoire CRISMAT, UMR 6508, CNRS/ENSICAEN, 6 boulevard du Maréchal Juin, 14050 Caen Cedex 4, France

Received April 17, 2008

The search for multifunctional materials as multiferroics to be applied in microelectronic or for new, chemically stable and nontoxic, thermoelectric materials to recover waste heat is showing a common interest in the oxides whose structures contain a triangular network of transition-metal cations. To illustrate this point, two ternary systems, Ba−Co−O and Ca−Co−O, have been chosen. It is shown that new phases with a complex triangular structure can be discovered, for instance, by introduction of Ga^{3+} into the Ba−Co−O system to stabilize $Ba_6Ga_2Co_{11}O_{26}$ and $Ba_2GaCo_8O_{14}$, which both belong to a large family of compounds with formula $[Ba(Co,Ga)O_{3-\delta}]_n[BaCo_8O_{11}]$. In the latter, both sublattices contain triangular networks derived from the hexagonal perovskite and the spinel structure. Among the hexagonal perovskite, the $Ca_3Co_2O_6$ crystals give clear evidence where the coupling of charges and spins is at the origin of a magnetocapacitance effect. In particular, the ferrimagnetic to ferromagnetic transition, with a one-third plateau on the $M(H)$ curve characteristic of triangular magnetism, is accompanied by a peak in the dielectric constant. A second class of cobaltites is the focus of much interest. Their 2D structure, containing CoO_2 planes isostructural to a CdI_2 slice that are stacked in an incommensurate way with rock salt type layers, is referred to misfit cobaltite. The 2D triangular network of edge-shared CoO_6 octahedra is believed to be responsible for large values of the Seebeck coefficient and low electrical resistivity. A clear relationship between the structures—incommensurability ratios—and the electronic properties is evidenced, showing that the charge carrier concentration can be tuned via the control of the ionic radius of the cations in the separating layers.

I. Introduction

For several decades, transition-metal (TM) oxides have been the focus of much attention, especially after the discovery of high-T_c superconductivity in layer cuprates.[1] In the latter, blocks of CuO_2 square lattice derived from the perovskite structure together with Cu^+/Cu^{2+} (n-type) or Cu^{3+}/Cu^{2+} (p-type) mixed valency of copper are responsible for the superconducting properties. Since then, the perovskite manganites $L_{1-x}A_xMnO_3$ and their derived 2D counterparts crystallizing in the Ruddlesden−Popper structures have been intensively studied for their colossal magnetoresistance.[2] For these manganites, the percolation of the magnetic-field-induced Mn^{3+}/Mn^{4+} ferromagnetic double-exchange regions in the localized charges of the antiferromagnetic matrix is responsible for the insulator-to-metal transition with a drop of the electrical resistivity, which could reach more than 10 orders of magnitude.[3] For all of these cuprates and manganites, the TMO orbital hybridation originates from the corner-shared TMO_x polyhedra of the mother $ATMO_3$ cubic perovskite. However, many other different connections between TMO_x polydedra also exist. In that respect, the cobaltites provide several of such examples as the structural family of "hexagonal" perovskites. Instead of stacking of the $[AO_3]$ layers as in the cubic $ATMO_3$ perovskite, these

* To whom correspondence should be addressed. E-mail: antoine.maignan@ensicaen.fr.

(1) Bednorz, J. G.; Müller, K. A. *Z. Phys. B* **1986**, *64*, 189.
(2) von Helmot, R.; Wecker, J.; Holzapfel, B.; Schultz, L.; Samwer, K. *Phys. Rev. Lett.* **1993**, *71*, 2331.
(3) Maignan, A.; Simon, Ch.; Caignaert, V.; Raveau, B. *C. R. Acad. Sci., Sér. IIb: Mec.* **1995**, *321*, 297.

10.1021/ic8006926 CCC: $40.75
Published on Web 09/29/2008

layers can be also stacked in a hexagonal way, leading to a structure made of chains of face-shared (TMO_6) octahedra all set on a triangular network such as for 2H-$BaCoO_3$.[4] Furthermore, the existence of oxygen-deficient stoichiometry corresponding to [$AO_{3-\delta}$] layers generates different kinds of polyhedra, allowing complex stackings to be generated as illustrated by the 5H or 12H hexagonal $BaCoO_{3-\delta}$ cobaltite (see ref 5 and references cited therein). In the following, we will review the structure of some cobaltites belonging to the Ca−Co−O and Ba−Co−O ternary systems. This will allow us to describe physical properties such as thermoelectricity or the magnetocapacitance (MC) effect related to the triangular nature of the cobalt cation lattices in all of these compounds.

II. Ca−Co−O Ternary System: $Ca_3Co_2O_6$ and $Ca_3Co_4O_9$

In the CaO−CoO phase diagram (in air) reported by Woerman and Muan in 1970,[6] two compounds corresponding to Ca/Co ratios of 3:2 and 3:4 were reported. By using KCO_3 or $SrCl_2$ as a flux in addition to the $CaCO_3$ and Co_3O_4 precursors, crystals of these phases have been grown.[7,8] Their morphology, needle- or plateletlike for $Ca_3Co_2O_6$ or $Ca_3Co_4O_9$, respectively, strongly suggested very different structural natures.

II.1. $Ca_3Co_2O_6$: An Ising Magnetic System on a Triangular Lattice. This compound is isostructural to Sr_4PtO_6,[9] a structure related to the hexagonal perovskites. As mentioned in the Introduction, the "−A−B−A−B−" hexagonal stacking of the [AO_3] layers yields the 2H hexagonal perovskite of the $A_3B_3O_9$ formula. This stacking mode creates octahedral crystallographic sites that are occupied by B cations, leading to the oxygen stoichiometric 2H-$BaCoO_3$ compound (Figure 1a,b). By considering a A_3O_9 unit obtained by tripling the [AO_3] layer and also by the removal of three oxygen anions, a A_3O_6 layer can also be built. So, in addition to the octahedral site created by the stacking of A_3O_9 units, the stacking of the A_3O_6 units generates a trigonal prism site occupied by a A′ cation. Finally, by mixing of the [A_3O_9] and [$A_3A'O_6$] blocks, a large family of oxides with general formula $A_{3n+3m}A'_nB_{3m+n}O_{9m+6n}$ (**1**) can be described, where the ratio between the [$A_3A'O_6$] and [A_3O_9] blocks is given by n/m.[10] For these compounds, the unit cell $a \sim 10$ Å corresponds to $\sim a_{H\sqrt{3}}$, where a_H is the hexagonal a parameter, and along the $\vec{c}$ axis, the structures can be described as chains of face-shared octahedra and trigonal prisms, occupied by the B and A′ cations, respectively. This is consistent with the needlelike aspect of the crystals. From **1**, the two first members for these cobaltites are 2H-$BaCoO_3$ ($m = 1$, $n = 0$; Figure 1a,b) and $Ca_3Co_2O_6$ ($m = 0$, $n = 1$; Figure 1c,d). In the latter, the chains set on a triangular lattice are made of 1:1 alternation of a CoO_6 octahedron (oct) and a trigonal prism (TP); these chains are separated by Ca^{2+} cations. Interestingly, as shown by X-ray absorption spectroscopy and magnetic dichroism, both oct and TP sites are occupied by a trivalent cobalt species but with distinct spin states, low spin ($S = 0$) and high spin ($S = 2$) in the oct and TP sites, respectively.[11] The strong anisotropy parameter, for $(Co^{3+})_{TP}$, $D \sim 150$ K,[12] gives an Ising-like character for the magnetization of the ferromagnetic chains in that compound, whereas the triangular networks of these antiferromagnetically coupled chains create a very frustrated magnetic system (Figure 1e), leading to remarkable magnetization jumps on the magnetization hysteresis loop of that compound.[13]

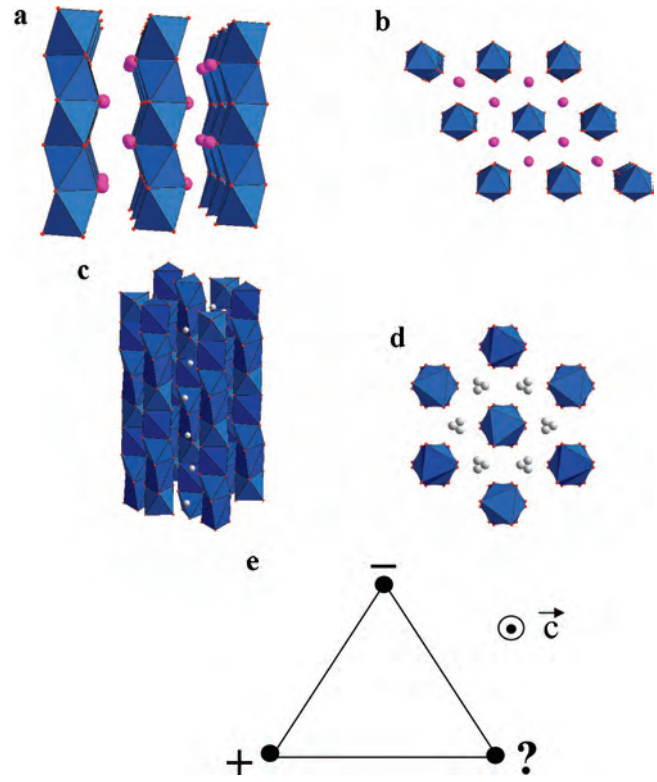

Figure 1. (a) ($\vec{a}$, $\vec{c}$) projection of the 2H-$BaCoO_3$ structures showing the chains made of face-shared CoO_6 octahedra separated by the Ba^{2+} cations (circles). (b) Corresponding ($\vec{a}$, $\vec{b}$) projection reveals the triangular lattice of the CoO_6 chains. (c) Perspective view of the $Ca_3Co_2O_6$ structure showing the chains of face-shared CoO_6 trigonal prisms and octahedra. The circles are for the Ca^{2+} cations separating these chains (d). The corresponding ($\vec{a}$, $\vec{b}$) projection is also shown together with the projection of the chain magnetization (e) to illustrate the magnetic frustration.

II.2. $Ca_3Co_4O_9$: A Complex Structure from an Apparent Simple Chemical Formula. The plateletlike morphology of these crystals is related to the 2D crystallographic structure

(4) Taguchi, H.; Takeda, Y.; Kanamaru, F.; Shimada, M.; Koizumi, M. *Acta Crystallogr., Sect. B: Struct. Crystallogr. Cryst. Chem.* **1977**, *83*, 1299.
(5) Panas, M.; Varela, A.; Seehofer, H.; Gonzalez-Calbet, J. M. *J. Solid State Chem.* **1995**, *120*, 327.
(6) Woermann, E.; Muan, A. *J. Inorg. Nucl. Chem.* **1970**, *32*, 1455.
(7) Lambert, S. Ph.D. Thesis, Caen University, Caen, France, 2002.
(8) Masset, A. C.; Michel, C.; Maignan, A.; Hervieu, M.; Toulemonde, O.; Studer, F.; Raveau, B.; Hejtmanek, J. *Phys. Rev. B* **2000**, *62*, 166.
(9) Fjellvag, H.; Gulbransdsen, E.; Aasland, S.; Olsen, A.; Hanback, B. *J. Solid State Chem.* **1996**, *124*, 190.
(10) Stitzer, K. E.; Darriet, J.; Zür-Loye, H. C. *Curr. Opin. Solid State Mater. Sci.* **2001**, *5*, 535.
(11) Burnus, T.; Hu, Z.; Haverkort, M. H.; Cazar, J. C.; Flahaut, D.; Hardy, V.; Maignan, A.; Brookes, N. B.; Tanaka, A.; Hsich, H. H.; Lin, H. J.; Chen, C. T.; Tjeng, L. J. *Phys. Rev. B* **2006**, *74*, 245111.
(12) Hardy, V.; Flahaut, D.; Frésard, R.; Maignan, A. *J. Phys.: Condens. Matter* **2007**, *19*, 145229.
(13) Maignan, A.; Michel, C.; Masset, A. C.; Martin, C.; Raveau, B. *Eur. Phys. J. B* **2000**, *15*, 657.

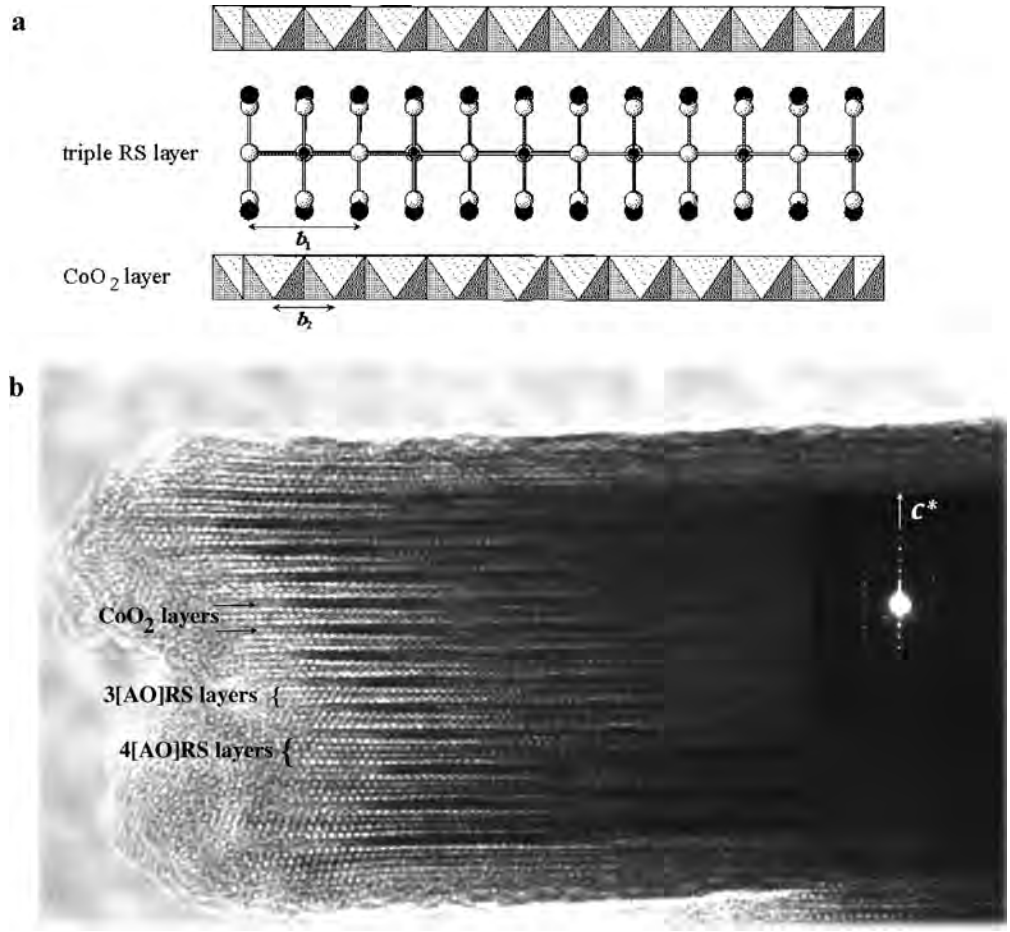

Figure 2. (a) Schematic structure of $[Ca_2CoO_3]^{RS}[CoO_2]_{1.61}$. (b) Example of a stacking of the CoO_2 layer (CdI_2-type) with three or four layers of the rock salt (RS) type observed from high-resolution electron microscopy.

(Figure 2a), which belongs to a broad family of the so-called "misfit" cobaltites. To elucidate this complex structure, the combination of transmission electron microscopy and X-ray diffraction has been determined.[8] The reconstruction of the reciprocal space from electron diffraction patterns revealed the coexistence of two monoclinic subsystems with common a, c, and β parameters but incommensurate b unit-cell parameters, which justified the "misfit" qualifier. Furthermore, the coupled energy-dispersive X-ray spectroscopy indicated a deviation from the reported Ca/Co = 0.75 ratio toward Ca/Co = 0.77. Accordingly, the structural refinement from X-ray diffraction patterns allowed one to propose the formula $[Ca_2CoO_3]^{RS}[CoO_2]_{1.61}$, where RS refers to the block of rock salt type layers separating CoO_2 layers crystallizing in the CdI_2-type structure. The subscript "1.61" corresponds to the incommensurability ratio b_1/b_2 between the b_1 and b_2 unit-cell parameters, with 1 and 2 standing for the RS and CoO_2 block layers, respectively. The hexagonal (H) CdI_2-type structure is related to the a and b_2 parameters according to the relations $a \sim a_{H\sqrt{3}}$, and $b_2 \sim a_H$. This hexagonal component consists of a CoO_2 layer isostructural to that of Na_xCoO_2. It is remarkable that this structural type can also be described by the stacking of oxygen layers[14] in a way similar to the one used for describing the hexagonal perovskites. The stacking of two "O_3" layers creates a network of edge-shared octahedra occupied by Co^{3+}/Co^{4+} cobalt cations, the lattice of which is triangular.

One remarkable consequence of this layer structure on the physical properties is that it stabilizes the low-spin states of both Co^{3+} ($S = 0$) and Co^{4+} ($S = {}^1/_2$) cations, which precludes any strong magnetic ordering for that compound. This unique situation for the Co^{3+}/Co^{4+} mixed valency is believed to be responsible for the thermoelectric properties of the layer cobaltites. At room temperature, the power factor (PF) of $Na_{0.7}CoO_2$ ($PF = S^2/\rho$, where S and ρ are for the Seebeck coefficient and electrical resistivity, respectively, is used to qualify the thermoelectric performance of a material) was reported to be similar to that of Bi_2Te_3, the most used thermoelectric materials.[15] The advantage of thermoelectric oxides, compared to conventional thermoelectrics, lies in their chemical stability in air, which is opening new opportunities to transform waste heat into electricity. In the "CaCoO" misfit cobaltite, the separating layers of the RS block are made of three layers, [CaO−CoO−CaO], but several other terms of the general formula $[(AO)_n]^{RS}[CoO_2]_{b_1/b_2}$ exist, as illustrated by the high-resolution electron microscopy (HREM) image shown in Figure 2b, and have been isolated (n varies from $n = 2$ to $n = 4$; A = Tl, Hg, Bi, alkaline earth, lanthanide). Among them, the

(14) Braconnier, J. J.; Delmas, C.; Fouassier, C.; Hagenmuller, P. *Mater. Res. Bull.* **1980**, *15*, 1797.

(15) Terasaki, I.; Sasago, Y.; Uchinokura, K. *Phys. Rev. B* **1997**, *56*, 12685.

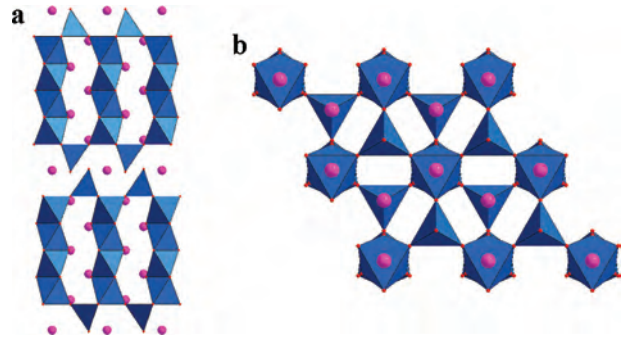

Figure 3. $(\vec{a}, \vec{c})$ projection of the 12H-$BaCoO_{2.6}$ structure (a) and corresponding $(\vec{a}, \vec{b})$ projection (b).

physics of the Bi-based members with four layers ($n = 4$), $[Bi_2A_2O_4]^{RS}[CoO_2]_{b_1/b_2}$, has been investigated in connection with the structural changes. This is discussed in section V together with the physical properties of a recently discovered rhodate with a new misfit structural type.

III. Ba−Co−O System: the New $[BaCoO_3]_n[BaCo_8O_{11}]$ Series

As discussed in the Introduction part, the cubic (c) or hexagonal (h) stacking of $[AO_{3-\delta}]$ layers allows us to describe the so-called hexagonal perovskites illustrated for the $BaCoO_{3-\delta}$ phases by the 2H (Figure 1) and 12H terms in Figure 3. The (a, b) plane projection of the former illustrates the triangular array of chains ($P6_3/mmc$ space group) made of the face-shared CoO_6 octahedra separated by the Ba^{2+} cations. It must be recalled that this compound is the ($m = 1$, $n = 0$) term of the $A_{3n+3m}A'_nB_{3m+n}O_{9m+6n}$ series with A = Ba and B = Co. In contrast to the 1D structure of the 2H structure (Figure 1a,b), the (a, b) projection (Figure 3b) of the 12H structure demonstrates that the units of four face-shared octahedra, reminiscent of the 2H chains, are bridged together by new types of CoO_x polyhedra resulting from the "$O_{2.6}$" oxygen deficiency. Consequently, by comparison of the 2H and 12H structures, it can be immediately deduced that the latter should exhibit a more 3D magnetic behavior. This is what is experimentally observed from the magnetic field magnetization curves collected at 2 K (Figure 4), showing a ferromagnetic behavior for the 12H term.[16] The presence of both ferromagnetism and mixed valency is also responsible for its negative magnetoresistance.[17] In fact, for the 1:1 ratio of Ba/Co, these hexagonal perovskites were identified in the $BaCO_3$−CoO phase diagram together with the phase Ba_2CoO_4 phase[18] and also the oxycarbonate $Ba_3Co_2O_6(CO_3)_{0.60}$.[19] In order to shift the Ba/Co ratio to values inferior to 1, attempts were made by incorporating Ga_2O_3 as one of the precursors. This was motivated by the discovery of new cobalt phases, brownmillerite Sr_2GaCoO_5,[20] and $(Ga_{1/3}Co_{2/3})_2Sr_2CoO_{6+\delta}$, isostructural to $Sr_4Fe_6O_{12+\delta}$,[21]

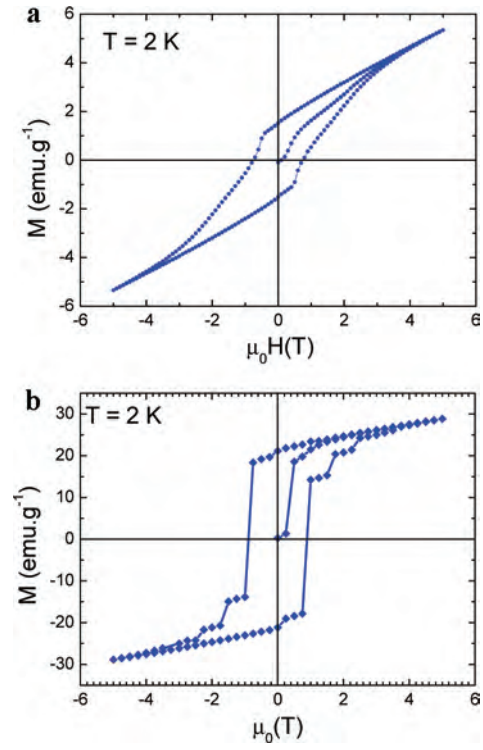

Figure 4. Magnetic field (H) dependence of the magnetization (M) collected at 2 K for the (a) 2H- and (b) 12H-$BaCoO_{3-\delta}$ compounds.

for which advantage was taken of the affinity of Ga^{3+} to form GaO_4 tetrahedral sites. As a result, two new phases crystallizing in a trigonal setting have been discovered, $Ba_6Ga_2Co_{11}O_{26}$[22] (Figure 5a) and $Ba_2GaCo_8O_{14}$[23] (Figure 5b). These new materials, isolated as single crystals, show strong structural relationships with the phases reported in refs 24 and 25. It must be emphasized that these plateletlike crystals show regular hexagonal shapes in good agreement with the observed symmetry groups. Here again, the structural study performed by combining X-ray diffraction and transmission electron microscopy has been necessary to solve the crystallographic structures. Besides a common layer block surrounded by ellipses in the projected views (Figure 5, right panel), these structures reveal an intergrowth with hexagonal perovskite blocks, 2H and 5H in $Ba_6Ga_2Co_{11}O_{26}$ and $Ba_2GaCo_8O_{14}$, respectively. Their common slab built from three layers corresponds to a "$BaCo_8O_{11}$" composition. Its central Co_4O_8 layer can be viewed as a Co_3O_8 kagome layer made of edge-shared CoO_6 octahedra encountered in the spinel structure in which the empty sites are occupied by a second type of cobalt. This central layer is sandwiched between two "$BaCo_2O_3$" layers built from top-shared CoO_5 tetrahedra and CoO_6 octahedra (Figure 5c). The general formula of these structures could be described by the general chemical formula $[Ba(Co,Ga)O_{3-\delta}]_n[BaCo_8O_{11}]$, where n

(16) Hébert, S.; Pralong, V.; Pelloquin, D.; Maignan, A. *J. Magn. Magn. Mater.* **2007**, *316*, 394.
(17) Maignan, A.; Hébert, S.; Pelloquin, D.; Pralong, V. *J. Solid State Chem.* **2006**, *179*, 1852.
(18) Boulahya, K.; Parras, M.; Gonzalez-Calbet, J. M. *J. Solid State Chem.* **1999**, *145*, 116.
(19) Boulaya, K.; Amador, U.; Parras, M.; Gonzalez-Calbet, J. M. *Chem. Mater.* **2000**, *12*, 966.
(20) Lindberg, F.; Istomin, Ya.; Berostegui, P.; Swensson, G.; Kazakovard, S. M.; Antipov, E. V. *J. Solid State Chem.* **2003**, *173*, 395.
(21) Pelloquin, D.; Hébert, S.; Pérez, O.; Pralong, V.; Nguyen, N.; Maignan, A. *J. Solid State Chem.* **2005**, *178*, 792.
(22) Pelloquin, D.; Pérez, O.; Martinet, G.; Hébert, S.; Maignan, A. *Chem. Mater.* **2007**, *19*, 2658.
(23) Martinet, G. Ph.D. Thesis, Caen University, Caen, France, 2007.
(24) Sun, J.; Yang, M.; Li, G.; Yang, T.; Liao, F.; Wang, Y.; Xiang, M.; Lin, J. *Inorg. Chem.* **2006**, *45*, 9151.

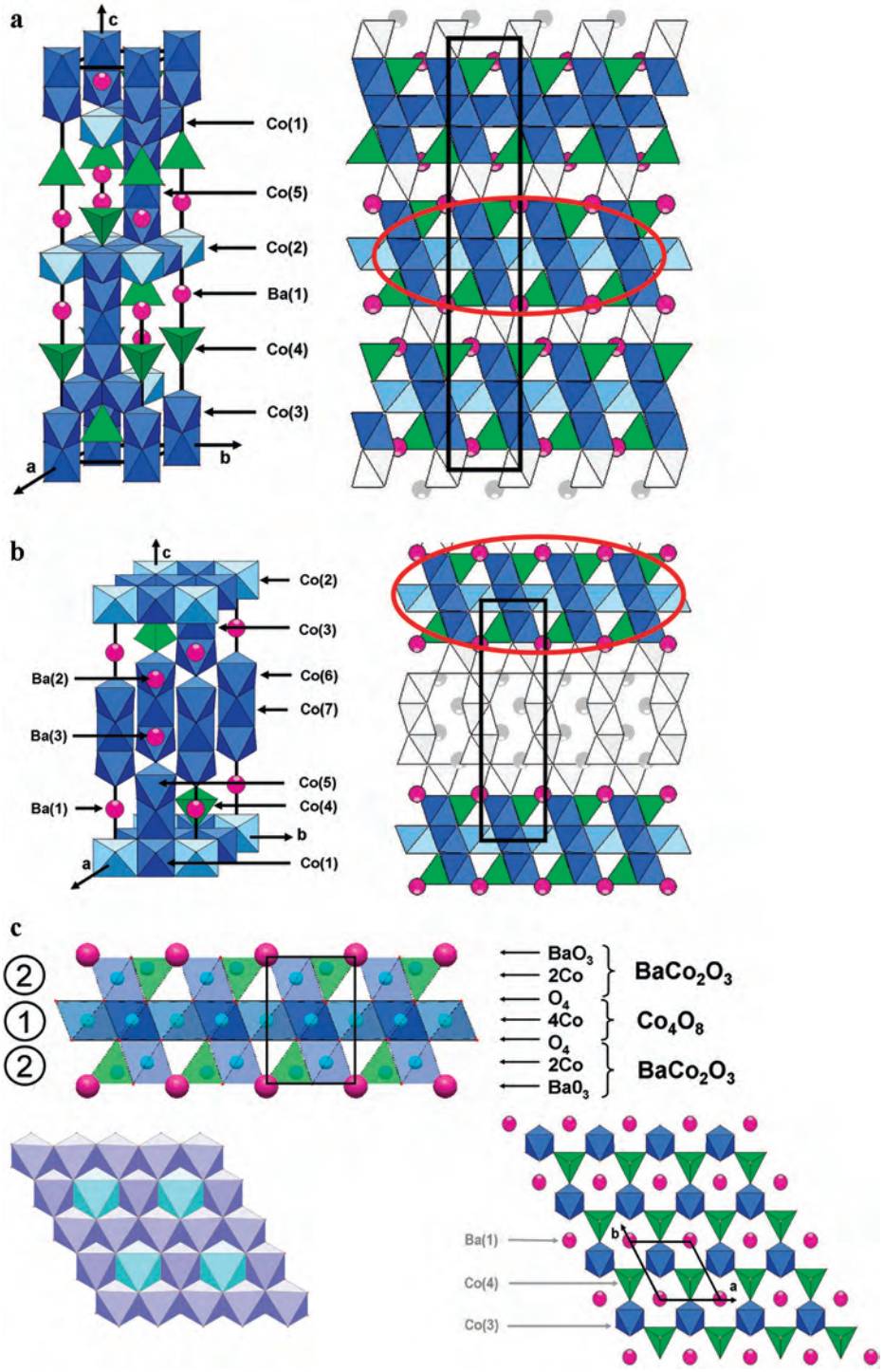

Figure 5. Perspective view and corresponding ($\vec{b}$, $\vec{c}$) projections of the oversimplified structures for $Ba_2GaCo_8O_{11}$ (a) and $Ba_6Ga_2Co_{11}O_{26}$ (b). For the ($\vec{b}$, $\vec{c}$) projections (right), the red ellipses show the existence of a common "$BaCo_8O_{11}$" block intergrown with units of the hexagonal perovskite layer. The central "$BaCo_8O_{11}$" block can be described by the stacking of a "Co_4O_8" (circled 1) derived from a "Co_3O_8" spinel layer with two $BaCo_2O_3$ (circled 2) layers (c).

refers to the thickness of the hexagonal perovskite unit. Thus, the periodicity along the stacking direction between two successive $BaCo_8O_{11}$ slabs can be tabulated as the formula 7 Å + n × 2.4 Å, leading to 19 and 9.4 Å for the n = 5 and 1 terms, respectively, i.e., in good agreement with the experimental c axis values of 18.82 Å (P-type lattice) and 29.15 Å (R-type lattice, ~3 × 9.4 Å).

These complex structures reveal how new structures can be generated by starting from an already studied phase diagram. Interestingly, the coexistence in these structures of $[CoO_2]$ planes, which can be viewed as isostructural to the conducting planes of Na_xCoO_2, together with blocks of hexagonal perovskites, which exhibit also various magnetic and electronic properties, opens opportunities to generate new properties.

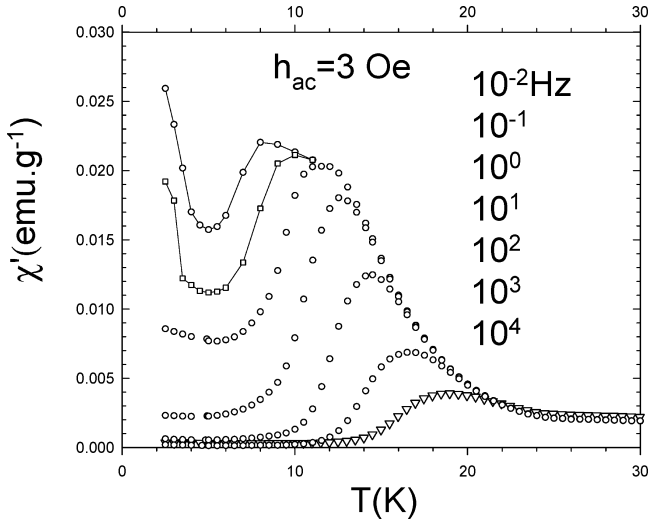

Figure 6. $Ca_3Co_2O_6$: real part of the magnetic ac susceptibility (χ') collected as a function of T for the different frequencies labeled in the graph. The h_{ac} magnetic field is applied along the magnetic chains direction (to the long dimension of the needlelike crystals).

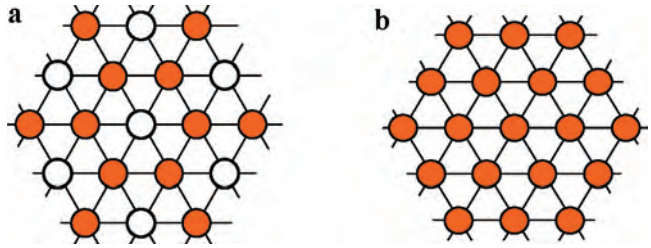

Figure 7. Schematic projections in a perpendicular plane of the chains magnetization of $Ca_3Co_2O_6$ below T_N showing a 2D triangular lattice of giant magnetic moments perpendicular to the plane (the filled and hollow circles are for the spin down and up, respectively). Two magnetic-ordered states are observed to be ferrimagnetic (a) and ferromagnetic (b).

In the following sections, two kinds of materials have been selected to illustrate their physical properties, an insulating magnetic one, $Ca_3Co_2O_6$, and the conducting layer Bi-based misfit oxides.

IV. $Ca_3Co_2O_6$: A Magnetodielectric Cobaltite

This ($m = 0$, $n = 1$) term of $A_{3n+3m}A'_nB_{3m+n}O_{9m+6n}$ exhibits a frustrated magnetism, which is examplified by its T dependence of the magnetic susceptibility (real part, χ'), showing a large shift of the χ' maximum as the frequency of the excitation magnetic field is increased (Figure 6). As a result, the magnetic ground state is the so-called "PDA",[26] for partially disordered antiferromagnetism, which is characterized by a one-third magnetization (M) plateau on the magnetic-field-dependent magnetization curves collected below $T_N = 25$ K. This indicates a transition from the ferrimagnetic structure (Figure 7a) to the ferromagnetic one (Figure 7b). The TP of the chains creates a strong uniaxial anisotropy, which forces the Co^{3+} magnetic moments to align parallel to the chains. In that crystallographic site, the observed orbital magnetic moment of high-spin Co^{3+},[11] suggesting a strong spin−orbit coupling, is responsible for a larger magnetic moment per cobalt than was expected for ferromagnetic high-spin Co^{3+} cations. Thus, it is expected that, upon external magnetic field application, this coupling will induce some structural changes that might affect the charge distribution in the materials. In other words, this would create a MC effect.

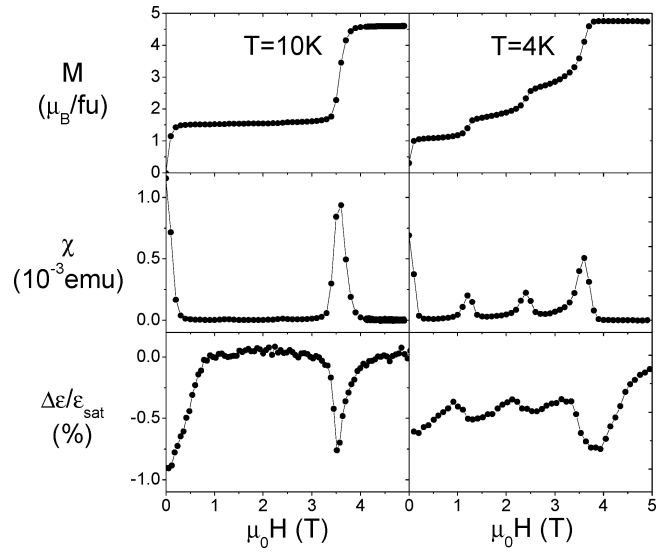

Figure 8. $Ca_3Co_2O_6$ isothermal ($T = 10$ K, left, and $T = 4$ K, right) magnetic field dependence of magnetization (M), magnetic susceptibility (χ), and $\Delta\varepsilon/\varepsilon_{sat}$.

In order to evidence such an effect, two large parallel faces of a needlelike crystal (3 mm in length with a diameter of ~200 μm) were covered with silver paste to apply an alternating current (ac) electrical field perpendicular to the chains. The magnetic field was applied along the long axis of the crystal to measure the MC. The T dependence of the complex impedance shows a clear decrease of the dielectric constant below T_N.[27] This already demonstrated that the charges and spins are coupled in that oxide. Furthermore, the isothermal measurements of an excess of the dielectric constant [$\Delta\varepsilon = (\varepsilon_H - \varepsilon_{sat})/\varepsilon_{sat}$] as a function of the magnetic field reveal a clear peak at about ~3.5 T and a broader peak starting from 0 T to about 0.8 T (ε_H and ε_{sat} correspond to the dielectric constant values measured for a magnetic field H and for H values saturating the magnetization, respectively; Figure 8). In fact, the shape of this curve mimics the $\chi(H)$ curve (χ is the magnetic susceptibility) obtained by derivation of the $M(H)$ curve (Figure 8). Finally, for lower T values ($T = 4$ K), the additional magnetization jumps on the $M(H)$ curve, regularly spaced by 1.2 T, are also detected by the MC measurements (Figure 8, right panel).

Such results demonstrate that insulating magnetic materials with competing magnetic interactions on a triangular array can be of interest for the search of new multifunctional materials. According to the numerous cobaltites crystallizing in structures favorable to the magnetic frustration, one might speculate that many properties have still to be discovered.

(25) Ehora, G.; Daviero-Minaud, S.; Colmont, M.; André, G.; Mentré, O. *Chem. Mater.* **2007**, *19*, 2180.
(26) Mekata, M. *J. Phys. Soc. Jpn.* **1997**, *42*, 76.
(27) Bellido, N.; Simon, Ch.; Maignan, A. *Phys. Rev. B* **2008**, *77*, 054430.

V. Misfit Cobalt Oxides: Example of the Bi-Based Misfit Cobalites and Rodhates

V.1. Misfit Cobaltite $[(AO)_n]^{RS}[CoO_2]_{b_1/b_2}$. A thermoelectric material is characterized by its dimensionless figure of merit $ZT = S^2T/\rho\kappa$, where T is the temperature, S the Seebeck coefficient, ρ the resistivity, and κ the thermal conductivity. The discovery of a large thermopower in the metallic Na_xCoO_2[15] has shown that, in these layered oxides, the figure of merit can be large. The misfits, because of the similar CdI_2-type layers, have therefore attracted a lot of interest.

Two models have been proposed to understand the large value of the Seebeck coefficient in these materials. First, Singh[28] calculated the band structure of Na_xCoO_2 and showed that, because of the trigonal symmetry, the t_{2g} orbitals are split into two families, a_{1g} responsible for metallicity and e'_g, with a peak at E_F, responsible for the large Seebeck coefficient. On the other hand, in a localized picture, the Heikes formula, which calculates the limit of S at high T, has been extended, taking into account the spin and orbital degeneracies of Co^{3+} and Co^{4+}[29] [$S = (-k_B/|e|)\ln\{g_3/g_4\}[x/(1-x)\}$ with x the Co^{4+} concentration], and large S are obtained because of the large spin and orbital degeneracies $g_3/g_4 = {}^1/_6$. However, this model should be applied only to localized carriers.

To investigate the importance of doping, the thermopower has been investigated in the misfit family, a material with the same CoO_2 layers but different block layers and in which the doping x in Co^{4+} can be adjusted by charge transfer between the two blocks. One key parameter in this system is the misfit ratio b_1/b_2 between the two block layers, and the Co valency in the CdI_2-like layers can be written as $v_{Co} = 4 - \alpha/(b_1/b_2)$, with α the positive charge of the NaCl-like layers. In the four-layer family ($n = 4$), the b_1/b_2 ratio can be modified from 1.67 for $[Bi_{1.7}Ca_2Co_{0.3}O_4][CoO_2]_{1.67}$ to 2 in $[Bi_2Ba_{1.8}Co_{0.2}O_4][CoO_2]_2$. The thermopower and resistivity of these different materials have been measured in polycrystals and single crystals. Figure 9 presents the $\rho(T)$ of single crystals and of a polycrystals and a single crystal of $[Ca_2CoO_3][CoO_2]_{1.61}$ (inset). The same trend is observed in $n = 3$ and 4. The difference between single crystals and polycrystals is mainly the value of resistivity, larger for polycrystals, emphasizing the importance of a good texturation of these materials to minimize ρ.[30] Above $T > 100$ K, a metallic behavior is obtained, with $\rho \sim 4-10$ mΩ cm at 300 K in single crystals. The smaller ρ is obtained for the larger b_1/b_2, i.e., in $[Bi_2Ba_{1.8}Co_{0.2}O_4][CoO_2]_2$. At low T, ρ strongly depends on the material. A strong increase of ρ is observed at low T for $[Bi_{1.7}Ca_2Co_{0.3}O_4][CoO_2]_{1.67}$, whereas ρ remains metallic with a T^2 behavior in $[Bi_2Ba_{1.8}Co_{0.2}O_4][CoO_2]_2$. Also, at low T a strong negative magnetoresistance is obtained in $[Bi_{1.7}Ca_2Co_{0.3}O_4][CoO_2]_{1.67}$,[31] in contrast with the positive magnetoresistance observed in the metallic $[Bi_2Ba_{1.8}Co_{0.2}O_4][CoO_2]_2$.[32]

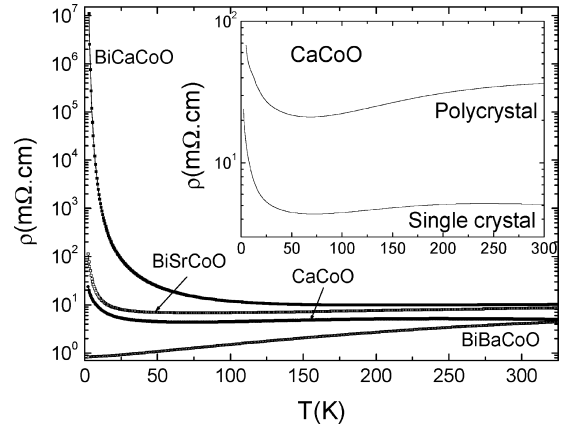

Figure 9. $\rho(T)$ of the $n = 4$ misfits BiCaCoO, BiSrCoO, and BiBaCoO. Also plotted is $\rho(T)$ of the $n = 3$ CaCoO. Inset: $\rho(T)$ of a polycrystal and a single crystal of CaCoO showing the lower electrical resistivity of crystals than polycrystals.

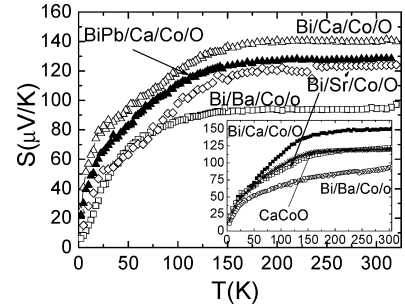

Figure 10. $S(T)$ of polycrystals of the $n = 4$ Bi-based misfit family and, in the inset, of single crystals of $n = 3$ and 4.

Figure 10 presents $S(T)$ values measured in different polycrystals. All curves present the same shape, with an increase of S up to ~100−150 K, followed by a plateau. The value of $S(T)$ at 300 K, $S_{300\ K}$, ranges from 90 to 140 μV K^{-1}. The same result is obtained for single crystals (inset of Figure 10), as was expected for thermopower measurements that are not sensitive to the microstructure of the materials. Also, for $[Ca_2CoO_3][CoO_2]_{1.61}$, the shape of $S(T)$ characteristic of the $n = 4$ family is observed, with an increase of S at low T, and a plateau at 120 μV K^{-1} for $T >$ 150 K. For the $n = 4$ family, when $S_{300\ K}$ is plotted as a function of b_1/b_2, a linear behavior is observed (Figure 11): the larger S is obtained for the smaller b_1/b_2, i.e., for the minimum Co^{4+} concentration. This result can be qualitatively explained by the Heikes formula, which states that the larger S is obtained for the smaller doping. Using directly the Heikes formula with $g_3/g_4 = {}^1/_6$, the Co valency would range from 3.5 to 3.7, much larger than the values obtained by other techniques, closer to 3.1−3.3.[33] Because of the complexity of the chemical formula, with possible oxygen nonstoichiometries, this value cannot be compared to the theoretical

(28) Singh, D. J. *Phys. Rev. B* **2000**, *61*, 13397.
(29) Koshibae, W.; Tsutsui, K.; Maekawa, S. *Phys. Rev. B* **2000**, *62*, 6869.
(30) Tani, T.; Itahara, H.; Xia, C.; Sugiyama, J. *J. Mater. Chem.* **2003**, *13*, 1865.
(31) Maignan, A.; Hébert, S.; Hervieu, M.; Michel, C.; Pelloquin, D.; Khomskii, D. *J. Phys. Condens. Matter* **2003**, *15*, 2711.
(32) Hervieu, M.; Maignan, A.; Michel, C.; Hardy, V.; Créon, N.; Raveau, B. *Phys. Rev. B* **2003**, *67*, 045112.
(33) (a) Brouet, V.; Nicolaou, A.; Zacchigna, M.; Tejeda, A.; Patthey, L.; Hébert, S.; Kobayashi, W.; Muguerra, H.; Grebille, D. *Phys. Rev. B* **2007**, *76*, 100403. (b) Bobroff, J.; Hébert, S.; Lang, G.; Mendels, P.; Pelloquin, D.; Maignan, A. *Phys. Rev. B* **2007**, *76*, 100407.

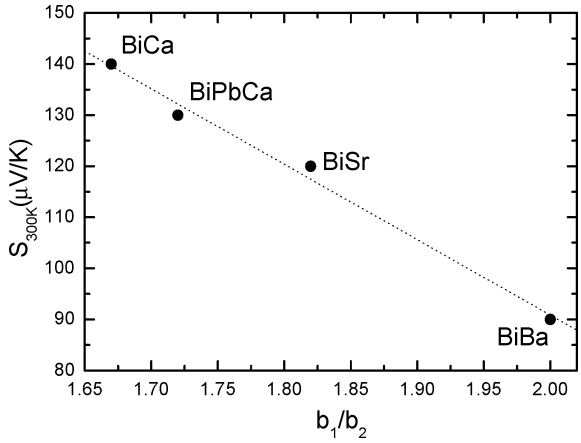

Figure 11. S measured at 300 K in polycrystals of the $n = 4$ family as a function of the incommensurability ratio b_1/b_2.

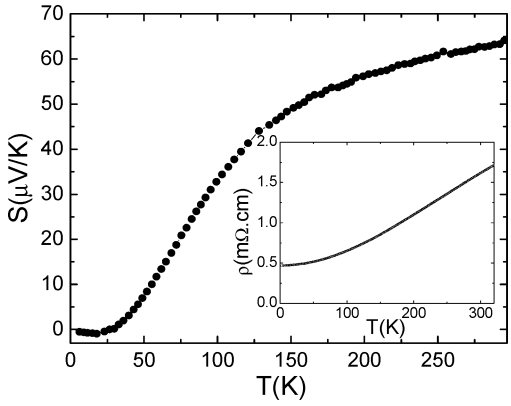

Figure 12. S(T) and $\rho(T)$ (inset) of $Bi_{0.78}Sr_{0.4}RhO_{3+\delta}$.

one, and other techniques are needed to probe the Co valency and compare it with the value obtained from the Heikes formula. Also, as shown by Limelette et al., the thermopower in $[Bi_{1.7}Ca_2Co_{0.3}O_4][CoO_2]_{1.67}$ can be separated into three contributions and the Heikes formula should not be directly applied to $S_{300\ K} = 150\ \mu V\ K^{-1}$.[34] Hall effect measurements have thus been performed on the single crystals[35] and confirm that doping increases when b_1/b_2 increases. The major result shown here is that the misfit ratio can tune the value of S at 300 K, by modifying the doping in the CoO_2 layers.

V.2. BiSrRhO: A New Family of Layered Rhodium Oxides. Single crystals of $Bi_{0.78}Sr_{0.4}RhO_{3+\delta}$ have been synthesized using a standard flux method.[36] Structural characterization by HREM and single-crystal X-ray diffraction is still in progress, but preliminary results show that this family consists of a complex intergrowth between a fluorite-type block and a Rh-based slice, with a trigonal symmetry.

The transport properties are shown in Figure 12. The resistivity (inset) is metallic, with a T^2 behavior characteristic of a Fermi liquid up to 120 K. The room temperature value is small, close to 1.6 mΩ cm at 300 K. In this metallic rhodium oxide, the thermopower is large, close to 65 μV K^{-1} at 300 K, and increases with temperature. The coexistence of these two properties is similar to what is observed in Na_xCoO_2.[15] PF $= S^2/\rho$ reaches 2.48 $\mu W\ cm^{-1}\ K^{-2}$ at 300 K, close to the values obtained in misfits. Hall effect measurements performed on these single crystals have shown that a large carrier density of $\sim 10^{22}\ cm^{-3}$ is obtained. As for misfits and Na_xCoO_2, this carrier concentration is much larger than the value obtained in classical thermoelectrics such as Bi_2Te_3 ($\sim 10^{19}\ cm^{-3}$ [37]). From the Hall effect measurements, the valency of Rh can be estimated to be close to 3.46. Following the extended Heikes formula (with $g_3/g_4 = 1/6$), a carrier concentration of $1.2 \times 10^{22}\ cm^{-3}$ is obtained in good agreement with the value obtained from the Hall effect. The smaller Seebeck coefficient may thus come from the larger concentration of carriers (here Rh^{4+}), compared to BiBaCoO. Nevertheless, the validity of the Heikes formula in this metallic system has to be determined, and high-temperature measurements are also required to determine the high-temperature value of S.

The striking similarities observed in this material, with a trigonal symmetry, with the misfits and Na_xCoO_2 show that a third family of metallic oxides with potentially good thermoelectric properties has been discovered. All of the properties can be understood as originating from CdI_2-like layers. If the CdI_2-like structure is confirmed by the structural analysis, this new family of layered oxides, with no structural misfit between the CdI_2 and block layers, and without Na^+ disorder, would help in an understanding of the importance of the block layer on the transport and magnetic properties in these layered oxides.

VI. Concluding Remarks

In this Forum Article, it is shown that cobaltites with crystalline structure made of Co-based triangular networks can exhibit many different kinds of electronic and magnetic properties.

In the compounds for which the magnetic Co−O chains are isolated from each other, such as in the 2H-$BaCoO_3$ and $Ca_3Co_2O_6$ phases, the magnetism is driven by a stronger intrachain magnetic coupling compared to the interchain one. Depending on the nature of the magnetocrystalline anisotropy, i.e., in the CoO_x polyhedron, the intrachain coupling can be ferromagnetic as in $Ca_3Co_2O_6$ in which high- and low-spin trivalent cobalt cations are respectively set in the trigonal prisms and octahedra, respectively. It is remarkable that the "high-spin" cobalt cations exhibit a magnetic moment larger than the theoretical one (4 μ_B), indicating a significant orbital magnetic moment aligned along the chain direction. The antiferromagnetic interchain coupling creates a frustrated situation at the origin of extra magnetization plateaus at low enough temperature on the magnetic-field-driven magnetization curve in addition to the one-third plateau characteristic of the triangular situation. It must be outlined that, in the 2H-$BaCoO_3$ compound also with CoO_6 chains but only octahedra, the lack of strong magnetocrystalline anisotropy

(34) Limelette, P.; Hébert, S.; Hardy, S.; Frésard, R.; Simon, Ch.; Maignan, A. *Phys. Rev. Lett.* **2006**, *97*, 046601.
(35) Kobayashi, W.; Muguerra, H., Hébert, S.; Grébille, D.; Maignan, A., to be published.
(36) Kobayashi, W.; Hébert, S.; Pelloquin, D.; Pérez, O.; Maignan, A. *Phys. Rev. B* **2007**, *76*, 245102.
(37) Mahan, G. D. *Solid State Phys.* **1998**, *51*, 81.

characteristic of the trigonal prism leads to a much weaker magnetism with no sign of long-range ordering. In that respect, the 2D character of the structures, derived from the 2H perovskites, with the chain units joined together by additional polyhedra, yields magnetic properties totally different from those of ferromagnetism in the 12H-$BaCoO_{2.60}$. Taking into consideration the MC properties found in $Ca_3Co_2O_6$, which is attributed to the spin−orbit coupling of the Co^{3+} lying in the trigonal prism, insulating phases recently discovered in the Ba−Co−O system are worth testing. This is also the case for other phases of the $A_{3n+3m}A'_nB_{3m+n}O_{9m+6n}$ system containing magnetic cations in the trigonal prism site A′.

The triangular 2D network of the TMs in the CdI_2-type layers provides another example of a large family of cobaltite with interesting properties. In those phases, the edge-shared CoO_6 octahedra favor low-spin states for both Co^{3+} and Co^{4+}, which are usually not observed in networks of corner-shared octahedra as in the structures derived from the perovskites. For instance, $La_{0.7}Sr_{0.3}CoO_3$ is ferromagnetic, whereas in the "misfit" cobaltite with similar Co^{4+}/Co^{3+} mixed valency, the magnetic ordering is not detected. As a result, the electrical resistivity is rather low for the oxides, with in-plane values of a few milliohm centimeters in the case of crystals of the Bi-based misfit cobaltites. The interest for such materials in thermoelectricity is related to the much larger charge carrier density than those of the classical thermoelectric materials, which are degenerate semiconductors. For sure, in the cobaltites, the resulting electronic correlations have to be considered to explain the rather large *T*-independent Seebeck values found in these materials, which is not expected in the case of a metal-like resistivity behavior. The similar behavior found in the case of rhodates with RhO_2 layers isostructural to CoO_2 confirms that the CdI_2 structural type is at the origin of these properties.

Thus, for chemists, structures containing triangular lattices appear to be very attractive candidates to generate new physical properties.

IC8006926